The Development of Quantitative Relationships between Orographic Precipitation and Air-Mass Parameters for Use in Forecasting and Cloud Seeding Evaluation

ROBERT D. ELLIOTT AND RUSSELL W. SHAFFER

Aerometric Research Inc., Santa Barbara Municipal Airport, Goleta, Calif.

(Manuscript received 6 November 1961, in revised form 12 January 1962)

ABSTRACT

The physical basis for a relationship between orographic precipitation and air-mass characteristics, wind flow pattern and gross terrain features is outlined. Consideration is also given to the manner in which the precipitation falls from cloud and is caught in a rain gage. A model is developed which is employed in conjunction with numerous storm sounding data to establish semi-empirical relationships between precipitation at four mountain stations in Southern California and upwind air-mass characteristics.

The sounding sites were several hours upwind of the mountain stations. This arrangement makes it possible to employ the relationships established for short term quantitative precipitation forecast purposes as well as for cloud seeding evaluation. It is believed that the general method employed is applicable in other climatic zones.

1. Introduction

There exists a great need for prediction procedures and associated observational networks adequate for the production of accurate, detailed, short-period quantitative precipitation forecasts in mountain areas. Such forecasts can form the basis for vital decisions in the management of flood control and water conservation facilities. These decisions, although not made frequently, nevertheless when made, can have long term repercussions on the welfare and economy of a whole region. Little is known concerning the forecast accuracy of existing procedures when applied to, say, hourly precipitation amounts in mountain areas, but it is safe to say it is quite low.

In addition, such forecast procedures could be employed effectively as a means for speeding up the evaluation of the results of weather modification projects by providing a basis for more sensitive statistical tests than are now available, a matter which is currently of paramount importance to the advancement of cloud-seeding technology.

In either application, the first requirement is to apply meteorological knowledge to the establishment of a quantitative relationship between orographic precipitation and pertinent measurable parameters. In the case of the forecasting application, there is an additional requirement that the relationships possess a time lag. The possibility that present meteorological knowledge applied to a mesoscale network which includes frequent rawinsonde observations (as frequent as one every three hours) could provide a basis for sufficiently accurate quantitative relationships to serve these purposes became evident in connection with a National Science Foundation sponsored storm study[1] in the Santa Barbara, California, area. One phase of this study is concerned with orographic precipitation on the Santa Ynez mountain range, an east-west oriented sharp ridge of 3500-ft to 4000-ft elevation paralleling the coast line. It lies about 5 mi inland and is separated from the coast by a narrow coastal plain several miles wide. Heavy orographic precipitation falls here as prefrontal southerly winds blow upslope. A similar analysis involving less frequent rawinsonde data but a larger number of storms was made for the San Gabriel range lying north of the Los Angeles Basin in connection with a special study for the Los Angeles County Flood Control District and reported on by North American Weather Consultants.[2] Here, again, the mountain ridge is oriented east-west. The crest line elevation averages 8000 ft with one peak over 10,000 ft. Fig. 1 shows the general geographical location of these two ranges.

In the Santa Ynez region rawinsonde information was available from Point Arguello, approximately 45 mi WNW of the precipitation gage area. In the San Gabriel region it was available from Santa Monica and Long Beach, approximately 45 mi SW of that gage area. This spatial separation of the measured orographic precipitation and the measured air-mass characteristics provided, because of the upstream location (with

[1] National Science Foundation Contract C104.

[2] North American Weather Consultants Report No. 15-2, 1961: Investigation of storm precipitation patterns of the Los Angeles River and San Gabriel River drainage basins and the shifts of the natural precipitation pattern produced by artificial nucleation. Goleta, Calif., 44 pp.

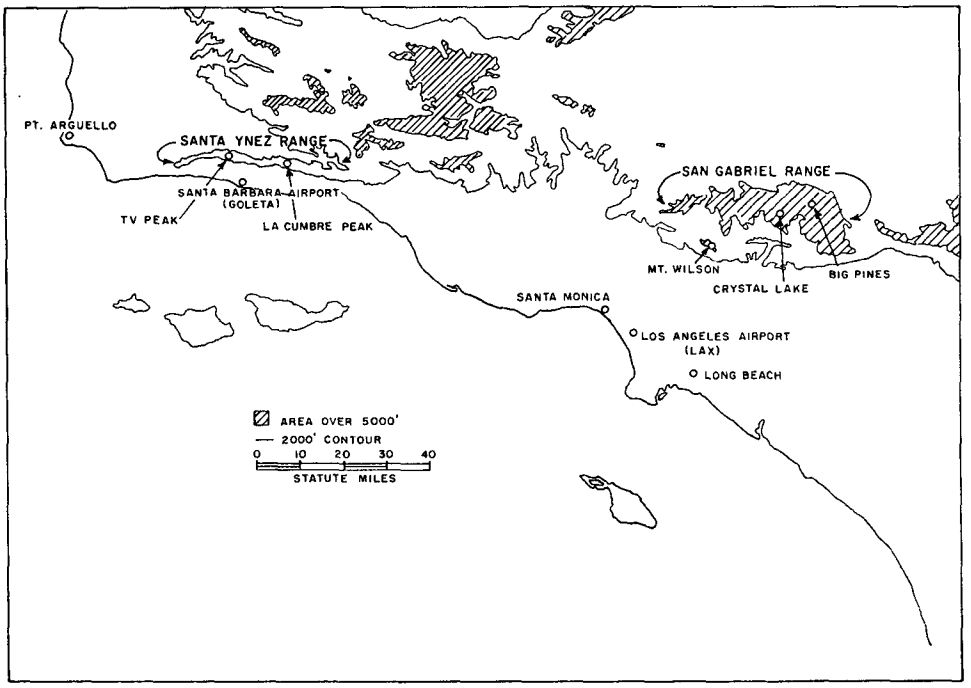

FIG. 1. Location of Santa Ynez and San Gabriel Ranges.

respect to system movement) of the sounding in both instances, a positive time lag of 1 to 5 hr, depending upon the speed of movement of the system. Therefore, this observational arrangement is ideally suited to the needs of short range quantitative precipitation forecasting.

2. Comparison of mountain and valley precipitation rates during storms

One of the well-known perplexing features of orographic precipitation patterns in the San Gabriel watershed, where a high rain gage density has existed for many years, is the great variability between storms in the ratio of high level mountain precipitation to coastal plain precipitation. Although in the majority of cases storms produce higher intensity precipitation in the mountains than in the coastal plains, the reverse is sometimes the case. This same phenomenon is also observed in the Santa Ynez range area. In both regions the coastal plains are flat and the precipitation regime is, aside from the minor effects of land-sea friction change, non-orographic in character. Therefore, the contrast between non-orographic and orographic precipitation is somehow involved. During the course of the Santa Barbara cloud seeding project the principal cause for these differences was revealed. Smith[3] demonstrates the role played by air-mass stability by comparing mountain precipitation rates to those observed in the Channel Islands during stable and unstable air-mass conditions. The mountain excesses occurred during the unstable regime.

Fig. 2 presents a time section of hourly precipitation amounts for an average of 3 mountain stations (Mt. Wilson, Crystal Lake and Big Pines) in the San Gabriels and for the coastal station at Los Angeles Airport (LAX). It is believed that this coastal station experiences a minimum of orographic effect. Data for three different storms are presented, each case representing a distinctive type from an assemblage of 7 yr of storm analyses, including most of the winter seasons from 1951–52 through 1959–60. The first storm is characterized by high intensity precipitation in the mountains relative to the coastal plain and by an air mass which is unstable (superadiabatic below the 750-mb level). The third storm represents the reverse case, namely, that of high intensity precipitation in the coastal plain relative to the mountains, and this occurred with a stable air mass. The second storm is a mixed type, the first part of which is characterized by relatively high plains precipitation rates and the longer enduring second part by relatively high precipitation rates in the mountains. The air mass shifted from stable to unstable as the character of the precipitation relationships changed.

The 7-yr sample showed that about two-thirds of the time precipitation in the San Gabriels is of the

[3] Smith, T. B., 1961: Physical studies of the Santa Barbara cloud seeding project. Meteorology Research Inc., Altadena, Calif., 22 pp.

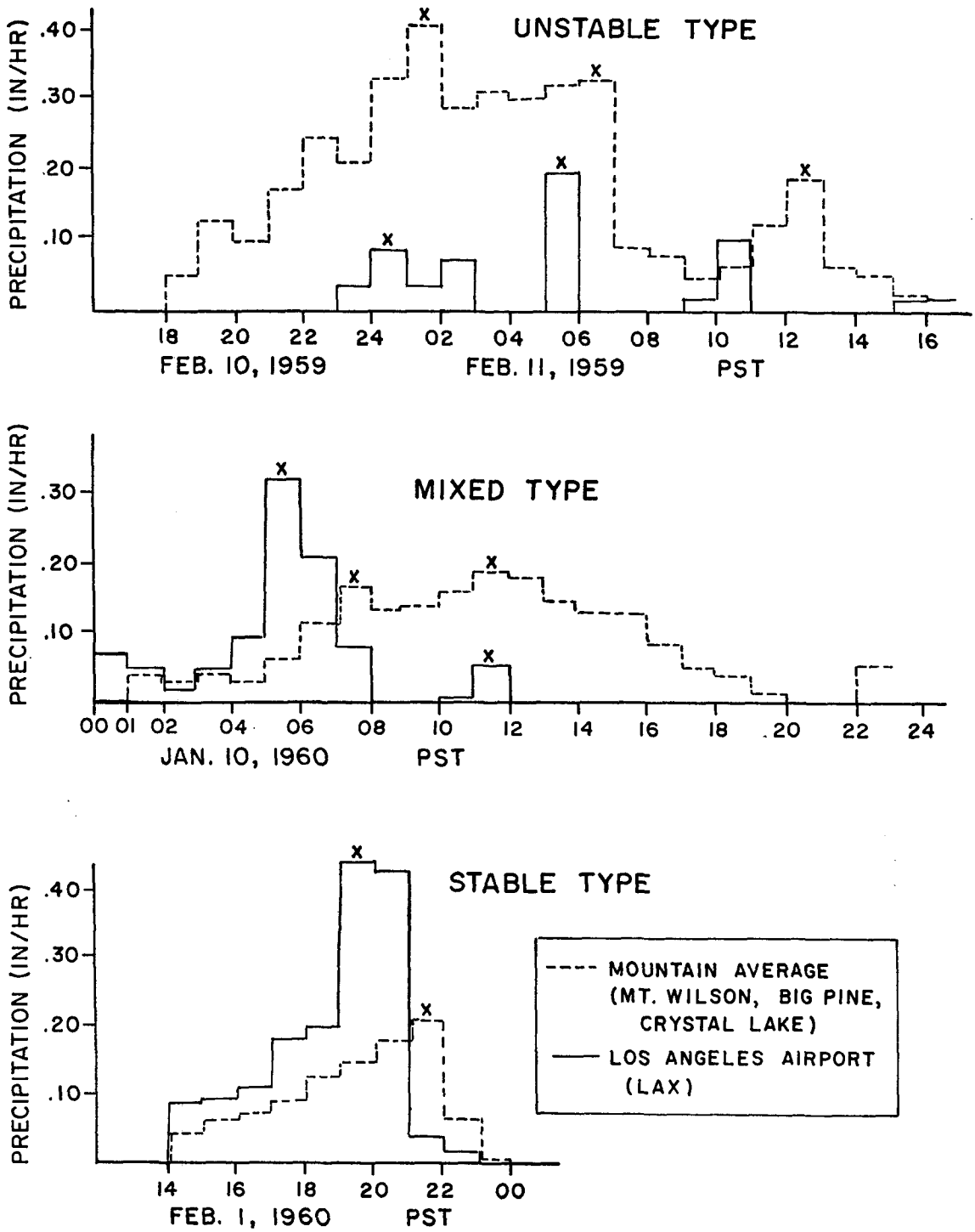

FIG. 2. Hourly precipitation rates, three types of storms.

unstable type and because of greater intensities with this type, approximately three-fourths of the mountain precipitation occurred during the unstable regime.

One universal feature of precipitation time sections such as these is the existence of occasional sharp peaks in hourly precipitation rates. These are denoted by X's in the figure. In these particular pluviographs, the peak time in the mountains generally occurs one to several hours following that in the plains and is associated with the passage of fronts and precipitation lines which can be traced through the area with considerable fidelity through detailed analyses of the numerous surface synoptic reports in the Los Angeles basin area. Thus, it would appear that frontal or precipitation line lifting does account for some of the mountain precipitation, but that apparently the bulk is accounted for by a purely orographic effect which can occur as a component added to the frontal lift, or separately as a completely independent process.

An example of the relationship between instability and precipitation is provided by Fig. 3 in which points are plotted for the Crystal Lake gage (a San Gabriel range gage at 5770-ft elevation) hourly precipitation total vs. LAX hourly precipitation totals for associated peak values over a 5-yr period. The outstanding features of this figure are, first, the extraordinarily high mountain to coastal plain precipitation ratio under some of the unstable cases and, second, the existence of a straight line lower envelope to the assemblage of points. This lower envelope was repeated for many high-level–low-level combinations in the San Gabriels and also in the Santa Ynez range. In all cases, the ratio of mountain to plains precipitation was less than one along the envelope. The interpretation of this observation is as follows:

Under very stable conditions, or conditions when the wind parallels the range, there is no significant orographic lifting, and precipitation is due entirely to frontal lifting. The amount is less in the mountains simply because the falling precipitation particles, which grow by collision and coalescence with cloud droplets, do not fall through as great a depth of cloud before reaching a high elevation rain gage as they do in reaching a low elevation gage. There are other factors having to do with gage catch characteristics which can also result in a reduction of recorded high level precipitation and these will be discussed later. The envelope is regarded as a direct measure of the non-orographic component of precipitation in the mountains. The amount by which the mountain precipitation exceeds that indicated for it by the envelope is therefore the orographic component of precipitation. Where time lag relationships between air-mass observations and orographic precipitation measurements are required for forecast purposes, the non-orographic precipitation should be measured at or near to the site of the soundings.

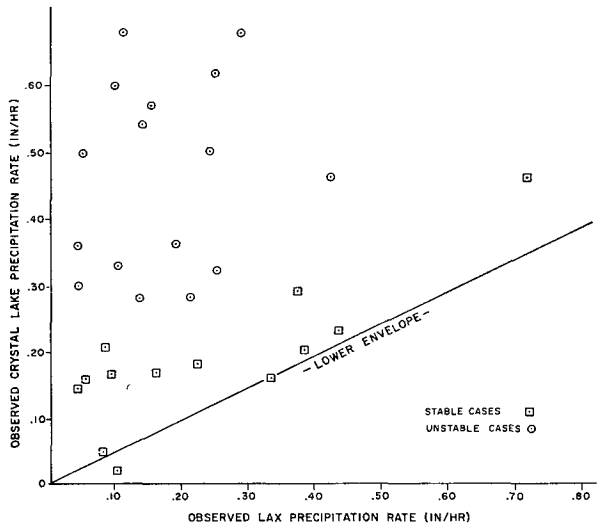

FIG. 3. Air mass, instability-stability and mountain vs. Los Angeles Airport hourly precipitation rates.

3. Air motion and precipitation particle fallout over an orographic barrier

An ideal forecasting model would make full use of basic meteorological knowledge concerning cloud physics and circulation on all scales. It would necessarily require as inputs measurements from an impossibly dense observing network. It is therefore necessary to formulate a compromise procedure based upon the existing temporal and spatial distribution of observations in these regions. After the forecast model is completed and tested, some rational estimates can be made as to what value might lie in increasing the network density.

A review of past models of orographic precipitation indicates two principal defects in them: first, the wind flow is apparently adapted too much to the stable case; and second, the cloud physics portion of the model is based upon the assumption that all of the condensed water falls out, and often that it falls directly down under the point of condensation.

Since no measurements are made directly of the air motion over the barrier, it is necessary to infer this flow from the soundings to the west. Therefore, a model for predicting the over-the-barrier airflow from the known undisturbed flow is needed. Models satisfying this condition specify a nodal surface at some elevation above the crest which serves as a lid to the orographic updraft. Two recent examples of this type of treatment are those of Knox[4] and Myers.[5] Myers' treatment is

[4] Knox, J. B., 1960: Procedure for estimating maximum possible precipitation. Bulletin #88, California Water Resources Department, 22 pp.

[5] Myers, V. A., 1959: Factors in California orographic rain. U. S. Weather Bureau, Washington, D. C., 16 pp. Paper presented at the 177th National Meeting of the American Meteorological Society at San Diego, Calif., 18 June.

particularly interesting in that he provides a procedure for determining the height of the nodal surface from wind and sounding data in the inflow section.

The basic equation employed by Myers is:

$$\frac{d}{dp}(v_0^2-v_i^2)=R(\gamma-\gamma_a)\ln p_i/p_o. \quad (1)$$

$\gamma-\gamma_a$ is the difference between observed lapse rate and that for adiabatic ascent. The subscript i refers to the inflow section, the subscript o to the outflow section, and v is the velocity and p the pressure on a given streamline. The geometrical pattern is made clear by Fig. 4. The observations available in our case presumably measure the inflow profile.

The term on the right represents the effect on kinetic energy distribution of the stabilizing force of the air mass. In the unstable condition this term is negative. Thus, the speed-up along a given streamline varies in the vertical if the term on the right differs from zero. Myers proposes that the air movement in the outflow section adjusts itself automatically to a minimum energy condition (approximately, minimum kinetic energy).

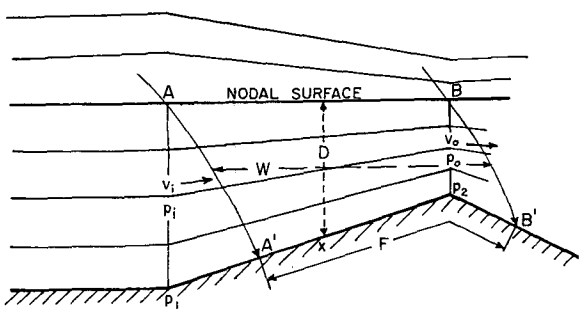

FIG. 4. Schematic diagram of air flow over an orographic barrier.

Since we shall be concerned with plus or minus variations about neutral stability, it is interesting to determine the height of the nodal surface in this instance. First, assume an inflow v_i which is uniform with height. Then integration of Eq (1) indicates, with the right side set equal to zero, that there is a uniform flow v_o at all heights in the outflow section and therefore that the outflow section kinetic energy is:

$$(KE)_o=\tfrac{1}{2}v_o^2(p_2-p_n), \quad (2)$$

where p_2 refers to the outflow ground level, and p_n to the nodal surface level. Continuity considerations indicate that:

$$v_o=v_i(p_1-p_n)(p_2-p_n)^{-1}, \quad (3)$$

where p_1 refers to the inflow at ground level pressure so that the above equation becomes:

$$(KE)_o=\tfrac{1}{2}v_1^2(p_1-p_n)^2(p_2-p_n)^{-1}, \quad (4)$$

where v_1 refers to the inflow ground level wind. From this it is found that the minimum kinetic energy occurs where:

$$p_1-p_n=2(p_2-p_n), \quad (5)$$

i.e., where the nodal surface is twice the barrier height in pressure units. It follows that under stable conditions the nodal surface will be below this level, and under unstable conditions, above it.

Vertical wind shear in the inflow region also influences the height of the nodal surface. Thus, if a simple vertical wind shear term is assumed such that: $v_i^2=v_1^2+\beta(p_1-p_i)$, then the integral of Eq (1) from ground level to p_i (or p_o) is:

$$v_o^2=v_2^2+\beta(p_1-p_i)+R(\gamma-\gamma_a)(p_2-p_o)(p_1-p_2)/p_2, \quad (6)$$

where v_2 refers to the outflow at ground level. In obtaining this result it is assumed that a satisfactory approximation to log x is given by $x-1$, and that the continuity equation is adequately represented by the approximation $(p_1-p_i)=v_2/v_1(p_o-p_2)$. It is also, of course, assumed that $\gamma-\gamma_a$ is constant through the layer. The outflow column kinetic energy from ground to nodal surface is then:

$$(KE)_o=\tfrac{1}{2}\int_{p_n}^{p_2}v_o^2dp_o=\tfrac{1}{2}\int_{p_n}^{p_2}[v_2^2+\beta(p_1-p_i)+R(\gamma-\gamma_a)(p_2-p_0)(p_1-p_2)/p_2]dp \quad (7)$$

which can be integrated with the help of the approximate continuity equation and becomes:

$$2(KE)_o=v_1^2(p_1-p_n)^2(p_2-p_n)^{-1}+\beta/2(p_1-p_n)^2+R/2(\gamma-\gamma_a)(p_2-p_n)^2(p_1-p_2)/p_2. \quad (8)$$

The minimum value of kinetic energy with respect to the nodal pressure p_n of this expression must be found to obtain the height of the nodal surface for minimum energy conditions. The final expression for p_n is a cubic and relates p_n to $\gamma-\gamma_a$ and β. Fig. 5 shows curves of height of the nodal surface against the stability index ΔT for no wind shear ($\beta=0$), and for a wind shear corresponding approximately to the relatively high value: 3 m sec^{-1} per 100 mb ($\beta=5\times10^3$). The stability parameter $\gamma-\gamma_a$ has been expressed in terms of the index ΔT which is the difference between observed 750-mb temperature and the temperature of adiabatic ascent to that level. It is seen that there is an abrupt rise in the nodal surface height as instability (negative ΔT) is achieved. The appearance of multiple values of p_n for a given stability in the unstable condition undoubtedly results from the approximations introduced into this derivation and is not real.

It should be noted that ΔT represents an index of mean air-mass stability and, in cases where the actual

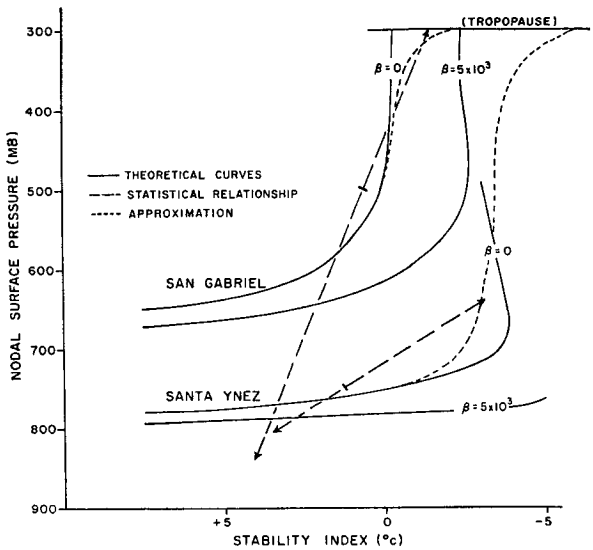

FIG. 5. Theoretical relationship of height of the nodal surface, stability and wind shear.

value of ΔT would indicate an unlimited depth of orographic updraft, the lifting will nevertheless be limited by the height of the tropopause and possibly also by other factors. The dotted lines in Fig. 5 represent a smoothing of the curve to accommodate this limit and also to correct for the approximation errors.

Attention will now be focused on the mechanics of condensation and precipitation. The reason for the existence of an orographic component of precipitation resides in the high condensation rate on the upwind slope beneath the nodal surface. It is in this moisture-rich zone that growth of fallout particles by collision and coalescence is greatly enhanced, and it is reasonable to assume that this enhancement is approximately proportional to the rate of condensation within the range of cloud types being considered. With this assumption, it becomes possible to construct a relatively simple model relating the orographic component of the precipitation to the various pertinent synoptic parameters. Fig. 4 contains in schematic form the essential parameters of this model. D is the depth of the orographic updraft pertaining to precipitation at point x, W the average width of the section scoured out by the falling particles, and F the length along which the precipitation is distributed. The area within which basically full orographic effect occurs is bounded on the sides by the limiting particle trajectories A-A′ and B-B′. The mean orographic updraft in this sector is very close to $\frac{1}{2}\ w_o$ or $\frac{1}{2}\ \bar{v}_i s$ where w_o is the orographic updraft at ground level, s is the smoothed mean slope and $\bar{v}_i$ is the mean inflow wind (normal to the mountain range orientation).

It is necessary to remark here that an extended mountain range may produce a large scale horizontal deflection of the basic airstream. Thus, an analysis of numerous pilot balloon observations taken along profiles from the Sacramento and San Joaquin valleys up to elevations of 7000 ft in the Sierra Nevada revealed that the winds below crest level back 40 deg as they approach the crest from the valley. It seems likely that this turning would be less with lower crest height, but nevertheless might be appreciable in the vicinity of the San Gabriel range, if not with the Santa Ynez.

It should also be remarked that the wind observations available do not truly measure the inflow wind, which has a strong southerly component. However, the horizontal homogeneity of the air mass over the flat terrain where the wind (and thermal structure) is observed is depended upon to make the measurements representative of the inflow air mass.

The mean interception rate (P_i) along F is given by:

$$P_i=\tfrac{1}{2}eKv_isDWF^{-1}, \tag{9}$$

where K represents the rate of condensation per unit of lift, and e is the fraction of the condensate which is removed as precipitation. The remainder presumably moves over the crest of the barrier as cloud droplets.

This equation merely relates the mean interception rate (of the orographic component of precipitation) to the mean condensation rate and is valid regardless of the precipitation mechanism (shower or non-shower type) provided the proper choice of bounding trajectories is made. Now the interception rate on the slope is merely the rate at which the depth of the precipitation would pile up in a vertical column. Conventional snow course depth measurements made with a snow core sampling tube give the accumulated interception directly. However, the rain gage measures a different quantity because it catches precipitation particles falling from different trajectory angles on a horizontal surface. It is seen from elementary considerations that the gage precipitation (P_g) will be:

$$P_g=(V_t-w_o)Nm, \tag{10}$$

where V_t is the particle terminal velocity, N the concentration of particles per unit volume and m the particle mass. This must be summed over the spectrum of actual particle sizes. Conceivably, the fallout trajectory could be horizontal ($V_t=w_o$) so that the gage catch is zero, but the sloping ground will still intercept precipitation.

Defining the interception rate as the rate of accumulation on the slope measured vertically, the geometry indicates that the interception rate is:

$$P_i=(V_t-w_o)Nm+v_iNms=P_g+v_iNms. \tag{11}$$

Here, s is the terrain slope and v_i the horizontal wind speed normal to the slope. Since $v_is=w_o$; $P_i=V_tNm$ so that the interception rate is proportional to the particle mass at the base of the trajectory. It can also

be seen that:

$$P_g = P_i(V_t - w_o)/V_t. \tag{12}$$

On the upwind slope, the greater the slope the greater will be the interception rate compared to the gage precipitation rate. Beyond the crest the downward motion reinforces V_t and the gage precipitation rate exceeds the interception rate. However, we shall be concerned with the upwind slope and the crest itself.

In addition, local effects such as are produced by terrain irregularities within 5 or 10 mi and very local disturbances produced by trees, bushes, or hummocks upwind of the gage, affect the catch. Where windflow is strong, as on the sharp crest of the Santa Ynez ridge, this effect may be extreme. A seasonal difference of one-third in the catch of two gages about 10 ft apart was found there by Court (1960). Although this represents a rather extreme case, it is interesting that such a marked local variation has been observed. Shields are often employed to increase catch of snow which, due to its low terminal velocity, has a flat trajectory. Here a very local effect over the gage itself is purposely created artificially to increase the catch.

Substituting into the above equation for the orographic component of precipitation one obtains:

$$P_g' = \tfrac{1}{2}(V_t - w_o)/V_t e K \bar{v}_i s D W F^{-1}. \tag{13}$$

P_g is primed as a reminder that it is the actual gage precipitation minus the non-orographic component of precipitation as determined for each station by the procedure outlined above in Section 2.

Theoretically $(V_t - w_o)/V_t$ is dependent upon the spectrum of drop size or snowflake shape, because of the relationship of sizes and shapes to terminal velocity. It is possible to evaluate this term, for various w_o values, by employing known characteristic raindrop distributions such as those given by Marshall and Palmer (1948) and other information on terminal velocities for raindrops (Gunn and Kinzer, 1949) and for snow (Langleben, 1954). Computations indicate that for heavy rain this factor varies from 0.6 to 0.8 for the smoothed mean slopes in question. On the basis of a long period of observation with many types of gages at the San Dimas Experiment Station in the San Gabriel range, Hamilton[6] found a ratio of gage catch to interception of 0.85.

Very little information is now available under any conditions concerning e, the fraction of condensate precipitated on the slope. Braham (1952) found a value of 0.19 for the summer thunderstorm. In a deep stable storm where natural nucleation is adequate and high cloud water content does not accumulate, e may be near to 1.0. An evaluation of this fraction was made for the Santa Ynez and San Gabriel data for numerous cases of near-neutral stability, where there is best assurance that the height of the nodal surface is twice the height of the barrier. The average precipitation observed over the profile minus the observed non-orographic precipitation measured at nearby flat terrain stations was compared to the computed condensation rate for the given orographic wind component. A mean value of 0.35 was found for the Santa Ynez and 0.67 for the San Gabriels.

K is a function of air-mass temperature as can be verified readily by reference to a standard adiabatic chart. A simple linear relationship holds in the vicinity of the sample mean air-mass temperature:

$$K = (0.730 + 0.093 H_f) \times 10^{-11}, \tag{14}$$

where H_f is the height of the freezing level in thousands of feet and K is in cgs units. This is a simple yet adequate index of air-mass temperature. It is pertinent to note here, in view of the use of surface dewpoint as a frequently used parameter in quantitative precipitation forecasting, that the variation in K with respect to temperature represents the variation in the moisture available for condensation of the air mass, if it is assumed that ceiling heights are the same for the warm and the cold air masses. This assumption has a basis in fact.

The variable $\bar{v}_i$ is measured only if there is no turning of the wind as the mountain range is approached from the observing site. Since it seems likely that there may be turning, it must be assumed that $\bar{v}_i$ is some simple function of the observed horizontal wind vector $\bar{v}_i$ and the angle ϕ between this and the normal to the range orientation.

The depth D, which is actually the height of the nodal surface minus the height of the gage (h_g), is not, of course, measured.

The terms W and s are both determined from the geometry of the barrier. However, F is a more complex matter. A large number of computations were made of fallout trajectories under various growth assumptions and it was determined that the difference between the ratio WF^{-1} and one would be small compared to other possible errors. Attention must also be given in selecting representative gages, to insuring that they do indeed lie in the zone F. The trajectory computations showed that with shower type precipitation such as occurs in the unstable cases where most of the precipitation falls as either high velocity heavily rimed particles or as large raindrops, the trajectories are quite steep.

In cold stable storms, however, the bulk of the precipitation falls as snow in dendritic form and has a very low terminal velocity. Under these conditions, it seems likely that a portion of the fallout trajectory lies upwind of the orographic updraft zone, thus effectively reducing WF^{-1}. The value of this ratio can conceivably fall as low as 0.7 in cold stable storms.

[6] Hamilton, E. L., 1954: Rainfall sampling on rugged terrain. Tech. Bull. No. 1096, U. S. Department of Agriculture, 41 pp.

The above discussion is summarized in Table 1 below:

TABLE 1. Summary of precipitation forecast parameters and their characteristics.

Parameters, some as functions of observed variables		Variations
$(V_t-w_0)/V_t$	(considered a constant 0.85)	0.60 to 0.85 Highest in warm deep storms
e	(considered a constant 0.35 Santa Ynez 0.67 San Gabriel)	Highest in cold deep storms
$K\approx f_1(H_F)$		$(0.730+0.093H_F)\times10^{-11}$
$v_i\approx f_2(v_0,\phi)$		$\bar{v}_i\cos(\phi+\lambda)$ where λ is probably under $\pm40°$ Local effects each gage can also be expected
$D\approx f_3(\Delta T,p_2,p_1,h_0)$		Fig. 5 relationships plus gage elevation
W/F	(considered a constant 1.0)	0.7 to 1.0 Highest in warm shallow storms

It is clear from the table that those parameters or combinations of parameters considered to be constants are indeed somewhat dependent upon temperature and depth, but that these variations are to some extent compensating. In the case of the variable parameters there exist functional relationships in which limited confidence can be placed. The effect of the wind is most uncertain due to the existence of relatively local effects.

Approximately, Eq 13 can be represented by:

$$p_0'=kD(\Delta T)K(H_F)(av_s+bv_w), \qquad (15)$$

where k is a constant for each gage, D a function of the measured parameter ΔT, K a function of the measured parameter H_F, and v_s and v_w are the observed mean southerly and westerly inflow wind components, respectively. a and b are the cosines of the angles between the components and the normal to the range.

This equation was employed to calculate the orographic component of gage precipitation rates at two stations in the Santa Ynez and at two in the San Gabriels. The observed ΔT was used with the Fig. 5 dotted curves to estimate the height of the nodal surface and from this was subtracted the gage height to obtain D. K was determined from Eq 14. Both ranges have a basic east-west orientation so that as a first approximation it was assumed that $a=1$, $b=0$. Rather than employing the mean wind, the value at the 5000-ft level at Long Beach or Santa Monica was used, and that at the 3000-ft level at Point Arguello. The latter level is rather high to represent a mean, but this choice was made in order to avoid surface friction effects.

The gage stations used on the crest of the Santa Ynez range were TV Peak, and La Cumbre Peak, both at 4000 ft. They are approximately 14 mi apart and their locations are indicated in Fig. 1. Data were taken from the period January through April 1960 with the addition of one storm in 1961. During this period 3-hr rawinsondes were available from Point Arguello. The two gage stations used in the San Gabriels were Crystal Lake at 5700 ft, and Big Pines at 6800 ft. Crystal Lake lies on the upwind slope and Big Pines just over the crest. At these latter stations the data were taken from seven years during which most of the soundings were 12 hr apart, with a few at 6-hr intervals and a number at 3-hr intervals in 1960. More details on available data appear in the North American Weather Consultants report.[7]

In the San Gabriel only the precipitation peaks were considered. Thus, the associated LAX and mountain area peaks such as those appearing in Fig. 2 were employed. It was therefore necessary to interpolate between soundings to obtain parameter values corresponding to the LAX precipitation peak time. Such interpolations were not made when the time to the nearest sounding was over 3 hr. In the Santa Ynez case all values were employed whether or not they fell on precipitation peaks.

Crystal Lake, Big Pines, TV Peak and La Cumbre were all influenced by cloud seeding in some storms during the sample period. These cases were deleted so that there can be no seeding effect in the computations.

Inasmuch as Eq 15 is actually a forecast equation, it is pertinent to remark briefly on the method used for establishing the time lag between the sounding and the mountain precipitation. This can be determined by mesoscale analysis of the movement of fronts and pressure change lines. As applied in this study it represents "hindcasting" rather than forecasting and may therefore provide a little more accurate timing than is possible in actual forecasting. The time lag between the coastal plains and the San Gabriels was normally

[7] North American Weather Consultants Report No. 15-2, 1961: Investigation of storm precipitation patterns of the Los Angeles River and San Gabriel River drainage basins and the shifts in the natural precipitation pattern produced by artificial nucleation. Goleta, Calif., 44 pp.

3 hr or more. During part of the 5 yr the soundings were taken at Long Beach Airport and during the remainder at Santa Monica. This change in location did not appreciably alter the time lag picture. Los Angeles Airport precipitation gage lines between them (see Fig. 1).

The time lags between the sounding site at Point Arguello and the Santa Ynez stations were also mostly about 3 hr. The "non-orographic gage" at the Santa Barbara Airport was, however, located in essentially the same time zone and therefore the formulae are not in this case strictly forecast formulae.

The correlation coefficients between the hourly orographic component of precipitation and that calculated by the above procedure ranged from 0.441 to 0.625. The absolute value of the precipitation in the San Gabriels was considerably lower than the prediction, indicating most probably that e was overestimated there.

An alternate approach which is plausible in view of the lack of precision in the estimates of various essential constants, is to deal with a linearized version of Eq 15. Expanding Eq 15 in a Taylor's series about mean values (barred) and dropping higher than first order terms, one obtains:

$$P_g' = K_1 + K_2(\Delta T - \overline{\Delta T}) + K_3(H - \bar{H}_F) + K_4(v_s - \bar{v}_s) + K_5(v_w - \bar{v}_w)$$

$$K_1 = (p_g')_m$$

$$K_2 = k\left[\overline{\frac{\partial D}{\partial \Delta T} K(av_s + bv_w)}\right] \qquad (16)$$

$$K_3 = k\left[\overline{D\frac{\partial K}{\partial H_F}(av_s + bv_w)}\right]$$

$$K_4 = k[\overline{DKa}]$$

$$K_5 = k[\overline{DKb}].$$

Approximate values of the constants K_2 through K_5 can be determined by employing information used above or, it is clear, empirical estimates of all five constants can be made from the precipitation data themselves by applying the method of least squares. It was decided to employ the latter approach and then to compare the derived constants with their theoretical values.

After computing the regression coefficients for each of the stations, the residual error was compared to each predictor parameter in order to ascertain whether higher order terms appear in the statistics. None appeared with respect to ΔT nor with respect to H_F. However, higher order terms were quite evident in the case of the wind terms. A plot of the residual error at each station was made upon a polar coordinate wind diagram. The rather striking patterns thus revealed will be discussed below. Finally, the smoothed error contours were drawn on these diagrams and employed at each station to form a final correction to the forecast as given by the multiple regression formula. Quite similar wind corrections were found to exist for the Eq 15 calculations.

4. Discussion of results

Table 2 summarizes the formulae statistics for each station. R is the correlation coefficient between the observed orographic component of precipitation and that calculated by Eq 15. R_m is the correlation coefficient between the observed orographic component of precipitation and the rates calculated by the regression formulae of the type of Eq 16. When the wind correction is made, the correlation coefficient is R_f. Finally, the correlation R_f' between the actual observed mountain precipitation and that calculated by the regression and wind correction method plus the non-orographic component as calculated by the method outlined in Section 2 is given.

TABLE 2. Summary of formulae statistics.

Gage	R	R_m	R_f	R_f'	K_2	K_3	N
Crystal Lake	0.494	0.803	0.826	0.939	−0.0732	0.0314	22
Big Pines	0.550	0.628	0.652	0.812	−0.0409	0.0170	21
TV Peak	0.441	0.691	0.773	0.899	−0.0296	0.0365	16
La Cumbre	0.625	0.536	0.600	0.667	−0.0193	0.0045	17

A steady increase in correlation is to be noted in reading from left to right. First, the linear regression formulae showed a closer relation to the orographic precipitation component than did the theoretical equation, except at La Cumbre. Whether this could be expected to continue with application to an independent sample remains in question. A second improvement is noted when the wind correction factor is employed. Finally, the comparison between the final calculation of total mountain precipitation and observed values shows a substantial correlation and it can be inferred that the section 2 method for computing the non-orographic contribution to mountain precipitation does indeed do so.

The following two columns contain the regression coefficients for the parameters: ΔT and H_F. The theoretical coefficient for H_F was computed to be +0.010 for the Santa Ynez Range and +0.016 for the San Gabriels.

The average straight line curve defined by the regression coefficient for ΔT is plotted for each mountain range (dashed lines) in Fig. 5. It is seen that it has a slope roughly in accord with what might be expected from theory. The dashed lines in the figure extend through the range of observed values.

The final column gives the number of points used in each calculation. Because sounding data during storms are scarce, the limited sample available was not divided in order to provide an independent sample for further testing. No tests were made of the statistical significance of the contribution of each variable to the total since there was no question as to the physical importance of each variable.

The wind correction terms for each station appear in Figs. 6 through 9. A glance reveals two outstanding features common to these diagrams. The first is the appearance of a positive correction along a single axis, or direction. This means that when the rawin observation (taken upwind) indicates a wind from this direction, a positive correction is required. In each figure the mean direction of this axis is indicated by a long arrow. A short arrow represents the wind direction of maximum effect given by the wind term regression coefficients. Some differences between the two directions appear but are not considered significant.

The second feature is the distinctive negative maxima lying beyond 20 deg to the right and to the left of the axis and at 10 to 15 m sec^{-1} speed. Although the statistical evidence for such a pattern at a single station is weak, the similarity of appearance between stations is remarkable and lends weight to the expectation that the patterns are real. One would expect more variation between stations, particularly in the San Gabriel range where local terrain irregularities are more marked. It seems, however, that the direction of the axis is apparently the only feature unique at each station.

These distinctive non-linear wind effects suggest that as the air approaches the station from a direction away from that likely to produce maximum orographic lifting, there is a bending of the airflow to a direction more parallel to the range, thus reducing orographic updraft, condensation and precipitation. On the other hand, when the basic air current impinges directly upon the orographic slope, there is no bending. This

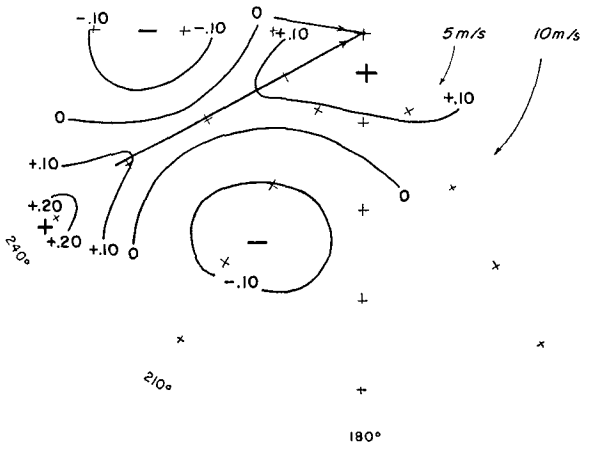

FIG. 6. Wind correction term—Crystal Lake.

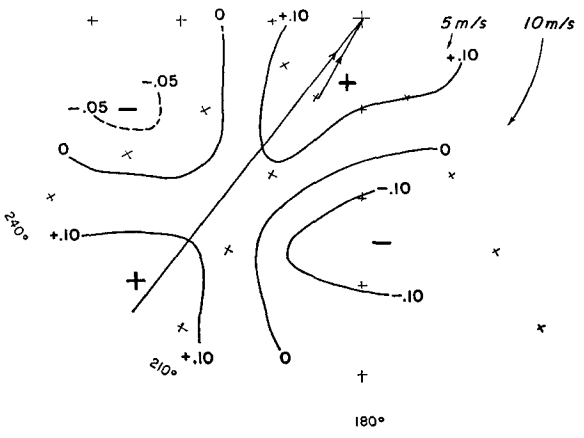

FIG. 7. Wind correction term—Big Pines.

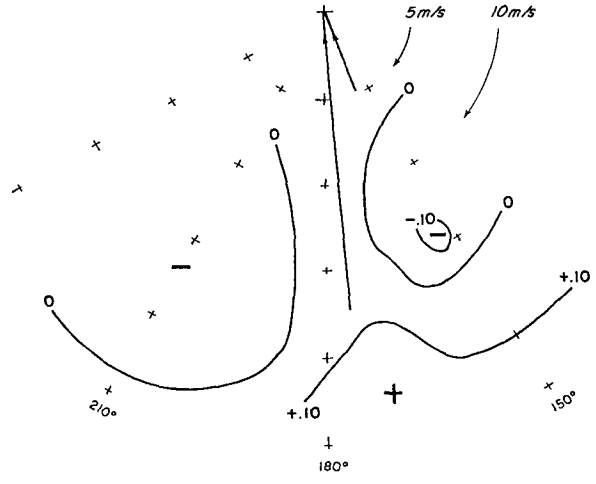

FIG. 8. Wind correction term—TV Peak.

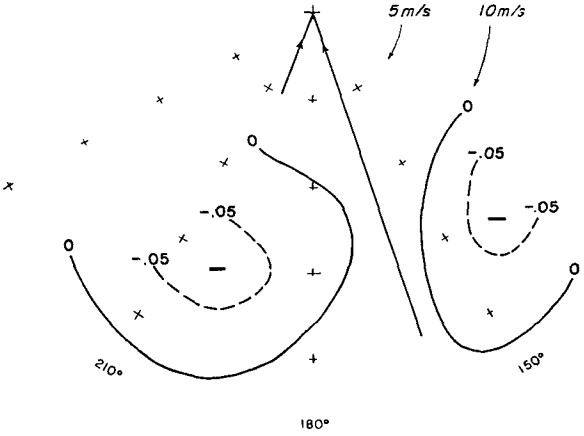

FIG. 9. Wind correction term—La Cumbre Peak.

effect is apparently a maximum for speeds of 10–15 m sec^{-1}. A heightening of the effect with increasing air mass stability might be expected on physical grounds, but the data sample was too small to warrant investigating this empirically.

5. Conclusions

The aforegoing approach to the orographic precipitation problem provides further evidence as to the crucial role played by air-mass instability. While the investigation has been confined to two mountain ranges lying not far from the Pacific Coast and south of 35N, it is believed that future studies will reveal the importance of these factors far inland and at more northerly latitudes. One might expect the instability effect to diminish to zero in much colder regions where the mountain radiational climate is colder than the actual climate.

From the practical viewpoint, it is believed that the effectiveness of a rational approach to the development of a short-range quantitative precipitation forecast procedure has been demonstrated. It turned out that fundamental meteorological knowledge was of most use in the selection of parameters. Nevertheless, something could also be provided for judging the reasonableness of the regression coefficients obtained by the statistical procedures. It should be emphasized that the results were based upon data from a dense network and that a sounding frequency of one every three hours, or even more frequent, would be desirable in order to obtain comparable or better relationships elsewhere.

The usefulness of such quantitative precipitation relationships in the evaluation of weather modification is obvious. The highest correlations possible are needed between observed and forecast (or hindcast) precipitation in order to have sensitive statistical tests.

The results suggest that more field studies and theoretical work should be done on wind flow on upwind mountain slopes under different conditions of air-mass stability. Actual observations of cloud top levels over flat and mountainous terrain are also needed.

Acknowledgments. The authors wish to thank the Los Angeles County Flood Control District for permission to use data from a special report to them. The National Science Foundation is thanked for their support of the basic data collection in the Santa Ynez area. Thanks are also due to Leona Sheldon for the computational work, Joyce Shea for the drafting and Louise d'Argastel for the typing of the manuscript.

REFERENCES

Braham, R. R., Jr., 1952: The water and energy budgets of the thunderstorm and their relation to thunderstorm development. *J. Meteor.*, **9**, 227–242.

Court, A., 1960: Reliability of hourly precipitation data. *J. geophys. Res.*, **65**, 4017–4024.

Gunn, R., and G. D. Kinzer, 1949: The terminal velocity of fall for water droplets in stagnant air. *J. Meteor.*, **6**, 243–248.

Langleben, M. P., 1954: The terminal velocity of snowflakes. *Quart. J. R. meteor. Soc.*, **80**, 174.

Marshall, J. S., and W. McK. Palmer, 1948: The distribution of raindrops with size. *J. Meteor.*, **5**, 165–166.